Detection of small drizzle droplets in a large cloud chamber using ultra high-resolution radar

Zeen Zhu[1], Fan Yang[1], Pavlos Kollias[1,2], Raymond A. Shaw[3], Alex B. Kostinski[3], Steve Krueger[4], Katia Lamer[1], Nithin Allwayin[3], Mariko Oue[2]

[1]Brookhaven National Laboratory, Upton, NY, USA
[2]Stony Brook University, Stony Brook, NY, USA
[3]Michigan Technological University, Houghton, MI, USA
[4]University of Utah, Salt Lake City, UT, USA

Corresponding author: Zeen Zhu (zzhu1@bnl.gov)

23 **Abstract**

25 A large convection cloud chamber has the potential to produce drizzle-sized droplets, thus offering

26 a new opportunity to investigate aerosol-cloud-drizzle interactions at a fundamental level under

27 controlled environmental conditions. One key measurement requirement is the development of

28 methods to detect the low concentration drizzle drops in such a large cloud chamber. In particular,

29 remote sensing methods may overcome some limitations of in situ methods.

30

31 Here, the potential of an ultra-high-resolution radar to detect the radar return signal of a small

32 drizzle droplet against the cloud droplet background signal is investigated. It is found that using a

33 small sampling volume is critical to drizzle detection in a cloud chamber to allow a drizzle drop in

34 the radar sampling volume to dominate over the background cloud droplets signal. For instance, a

35 radar volume of 1 cubic centimeter (cm^3) would enable the detection of drizzle embryos with

36 diameter larger than 40 μm. However, the probability of drizzle sampling also decreases as the

37 sample volume reduces, leading to a longer observation time. Thus, the selection of radar volume

38 should consider both of the signal power and the drizzle occurrence probability. Finally,

39 observations from the Pi Convection-Cloud Chamber are used to demonstrate the single drizzle

40 particle detection concept using small radar volume. The results presented in this study also

41 suggest new applications of ultra-high-resolution cloud radar for atmospheric sensing.

42

43

44

45

46

47

48

49

50

51

1. Introduction

53 Drizzle formation is one of the most important microphysical processes in warm clouds. Yet the
54 processes controlling drizzle formation remain poorly understood (Wood, 2012). The most
55 challenging aspect is the initial formation of drizzle embryos with diameter around $30\ \mu m \sim 50$
56 μm. The formation of small drizzle particles in this range can neither be adequately explained by
57 the traditionally-defined condensation growth process nor by the traditionally-defined collision-
58 coalescence (C-C) process owing to their low efficiency (Yau and Rogers, 1996). Several
59 mechanisms have been hypothesized to explain the efficiency of these processes including i) fine-
60 scale turbulence in cloud (Pinsky and Khain, 1997;Shaw, 2003); ii) giant cloud condensation
61 nuclei (GCCN) (Johnson, 1982;Feingold et al., 1999);   and iii) longwave cooling (Roach,
62 1976;Harrington et al., 2000). Nevertheless, it remains unclear to which extent these proposed
63 mechanisms can adequately explain the origin of drizzle embryos.

64 Two main barriers that hinder our ability to investigate the drizzle initiation process are our
65 inability to isolate various effects in a real cloud and the lack of observations with sufficient
66 sensitivity and spatiotemporal resolution to detect the early growth of drizzle particles. As such an
67 instrumented large convection cloud chamber with well-controlled initial and boundary conditions
68 might help to improve our understanding of the drizzle initiation mechanism (Shaw et al., 2020).
69 Unlike other types of chambers, a convection-cloud chamber can generate a steady state cloud
70 system for hours in a turbulent environment by maintaining a warm saturated bottom surface, a
71 cold saturated top surface, and a constant aerosol injection rate (Chang et al., 2016). The Michigan
72 Tech Pi convection chamber with a dimension of 2 m x 2 m x 1 m (width x depth x height) has
73 been used to explore aerosol-cloud-turbulence interactions, however, the Pi Chamber is too small
74 to initiate drizzle embryos mainly due to the relatively short lifetime of cloud droplets therein.
75 Results from large eddy simulations indicate that drizzle can be initiated in a large convection-
76 cloud chamber with a height on the order of 10 m (Thomas et al., 2023). However, the drizzle
77 drops are sparse in a large chamber, so the detection of single drizzle embryos in a large cloud
78 chamber is challenging for in-situ probes that generally have a sampling volume of only a few
79 cubic centimeters. On the other hand, active remote sensors have the ability to rapidly sample large
80 volumes and thus offer an attractive option for the detection of small drizzle droplets in a cloud
81 chamber.

82

83   Here, we will demonstrate that the detection of an individual drizzle droplet in the presence of

84   numerous cloud droplets is possible with a radar that can achieve a very small sampling volume.

85   The detection of individual drizzle droplets is possible because the radar signal-to-noise ratio (SNR)

86   of a point target (drizzle droplet) is not affected by the radar observational volume, while the SNR

87   of a distributed target (cloud droplets) scales with the radar volume. In the following sections, the

88   detection limits of an individual drizzle particle are investigated using idealized particle size

89   distributions and real particle size distributions from the Michigan Tech Pi Chamber. In the end,

90   the potential of THz radars offering unprecedented sub-centimeter range resolution will be

91   discussed for developing the single drizzle detection radar (Cooper and Chattopadhyay, 2014).

92

93

94

95   **2. Drizzle detection using radar**

96

97   The detection of early drizzle particles in clouds has been the topic of extensive research. First, the

98   radar needs to have sufficient sensitivity to detect cloud and drizzle droplets. This is typically

99   accomplished using millimeter-wavelength radar (Kollias et al., 2007). Early methodologies for

100   the detection of drizzle drop in clouds employ the use of reflectivity thresholds, ranging

101   from −15 to −20 dBZ, to identify drizzle existence (Frisch et al., 1995;Liu et al., 2008;Comstock

102   et al., 2004). Kollias et al. (2011) introduced the use of the radar Doppler spectra skewness as a

103   more sensitive method for detecting the presence of small drizzle droplets (Acquistapace et al.,

104   2017;Zhu et al., 2022). The radar Doppler spectra technique improved the detection of drizzle

105   droplets that can produce as low as -30 dBZ (Zhu et al., 2022).

106

107   However, the use of the radar Doppler spectra technique in a cloud chamber is challenging. First,

108   this will require that the radar point vertically to take advantage of the differential velocity between

109   cloud and drizzle droplets. If we assume a monodisperse droplet size distribution (DSD) and

110   Rayleigh scattering conditions, a drizzle detection limit of -30 dBZ is equivalent to a concentration

111   of 10^{-3} cm^{-3} of drizzle droplets with diameter equal to 100 μm or a concentration of 6.4×10^{-2}

112   cm^{-3} of drizzle droplets with 50 μm diameter. In the former case, the drizzle particle size is quite

113   large and not quite an early drizzle droplet detection. In the latter case, the concentration of drizzle

114   droplets is much higher than the concentration observed in nature ($\sim 10^{-4}\ cm^{-3}$) (Zhu et al., 2022).

115   Furthermore, the conventional cloud radar has range resolution of tens of meters, which is not

116   applicable in a chamber facility which may be on the order of several meters (approaching the

117   collision mean free path).

118

119   As a result, we consider alternative methods to increase the probability of early drizzle droplet

120   detection against the cloud droplet signal. As the number concentration of drizzle particle is low,

121   by applying a small radar sampling volume V_{Radar}, it is possible that only one drizzle droplet is

122   presence in V_{Radar}. In this case, the drizzle particle can be considered as a point target with

123   backscattering cross section $\sigma(m^2)$ and the received radar echo power P_r (mW) is commonly

124   expressed as (Battan, 1973):

125

126
$$P_{r,drizzle} = P_t \frac{G^2 \lambda^2}{(4\pi)^3 r^4} \sigma(D_d) \tag{1}$$

127

128   where P_t is the transmit peak power (mW), G is the antenna gain, r (m) is the range of the target

129   relative to the radar receiver and λ (m) is the radar wavelength. It is noteworthy that P_r for a point

130   target does not depend on the radar sampling volume V_{Radar}. For distributed targets such as a cloud

131   droplet population described by a droplet size distribution (DSD) that represents the number

132   concentration of cloud droplets as a function of diameter, the received radar echo power is given

133   by:

134

135
$$P_{r,cloud} = P_t \frac{G^2 \lambda^2}{(4\pi)^3 r^4} \cdot V_{Radar} \cdot \sum_{i=0}^{n} N_c(D_i)\sigma(D_i)\Delta D_i \tag{2}$$

136

137   Where n is the number of cloud droplets in the radar volume and $N_c(D)$ is the DSD with units of

138   m^{-4}. In this case, the received radar echo power depends on the radar sampling volume, which is

139   given by the following expression:

140
$$V_{Radar} = \pi \left(\frac{r\theta_{3dB}}{2}\right)^2 \cdot \Delta R \tag{3}$$

141

142   where θ_{3dB} is antenna radiation pattern 3-dB beamwidth in radians and ΔR is the range resolution.

143   Assuming Rayleigh scattering, the backscatter cross section of the drizzle and cloud droplets is

144   proportional to the sixth power of the particle diameter and inversely proportional to the fourth

145   power of the wavelength ($\sigma(D) \sim D^6/\lambda^4$). Combing Eq. 1 and Eq. 2, the ratio of radar received

146   echo power from drizzle and cloud is given by the following expression:

147

148
$$\frac{Signal}{Background} = \frac{P_{r,drizzle}}{P_{r,cloud}} = \frac{1}{V_{Radar}} \cdot \frac{D_d^6}{\sum_{i=0}^{n} N_c(D_i) D_i^6 \Delta D_i}. \quad (4)$$

149

150 Eq. 4 indicates that the probability of detecting a single drizzle droplet in the radar sampling

151 volume increases inversely to the radar sampling volume (point vs distributed target).

152

153   3. Detection requirement

154

155 Here, we will evaluate how small the radar sampling volume needs to be to detect drizzle drops

156 with different diameters against three background (cloud) conditions: i) monodisperse cloud DSD,

157 ii) cloud DSD from a theoretical model and iii) observed cloud DSD from the Michigan Tech Pi

158 Chamber. For simplicity, we will assume that a drizzle drop is detectable if its radar return power

159 is equal to that of the background echo contributed from cloud droplets.

160

161   3.1. Monodisperse cloud DSD

162

163 We first construct an idealized scenario by considering two categories of droplets, i.e. cloud droplet

164 with a diameter of D_c and a single drizzle drop with a diameter of D_d, the number concentration

165 of cloud droplets in the radar sampling volume is N_c (m^{-3}).

166

167 In this case, Eq. 4 is simplified as:

168

169

170
$$\frac{Signal}{Background} = \frac{1}{V_{Radar}} \cdot \frac{D_d{}^6}{N_c \cdot D_c^6}$$
(5)

171

172 When the signal power equals to the background, the radar sampling volume enabling single

173 drizzle particle detection is estimated as a function of the size ratio $x = \frac{D_d}{D_c}$ shown in Fig. 1. The

174 results are shown for various cloud droplet concentrations. It is noted that the required radar

175 volume for detection depends on the drizzle drop size and the cloud number concentration. Larger

176 radar volume would be required for drizzle detection as the particle size ratio increase; for a given

177 particle size ratio, decreasing cloud number concentration can enhance the required radar volume.

178 For example, if the cloud number concentration is 50 cm^{-3} and the mean cloud diameter (D_c) is

179 20 μm, then the detection of a drizzle particle with diameter of 40 μm ($x = 2$) requires radar

180 volume around 1 cm^3. Such sampling volume are not achievable with traditional radar systems

181 that employ sampling volumes of the order of 1000 m³ or more (Kollias et al., 2016).

182
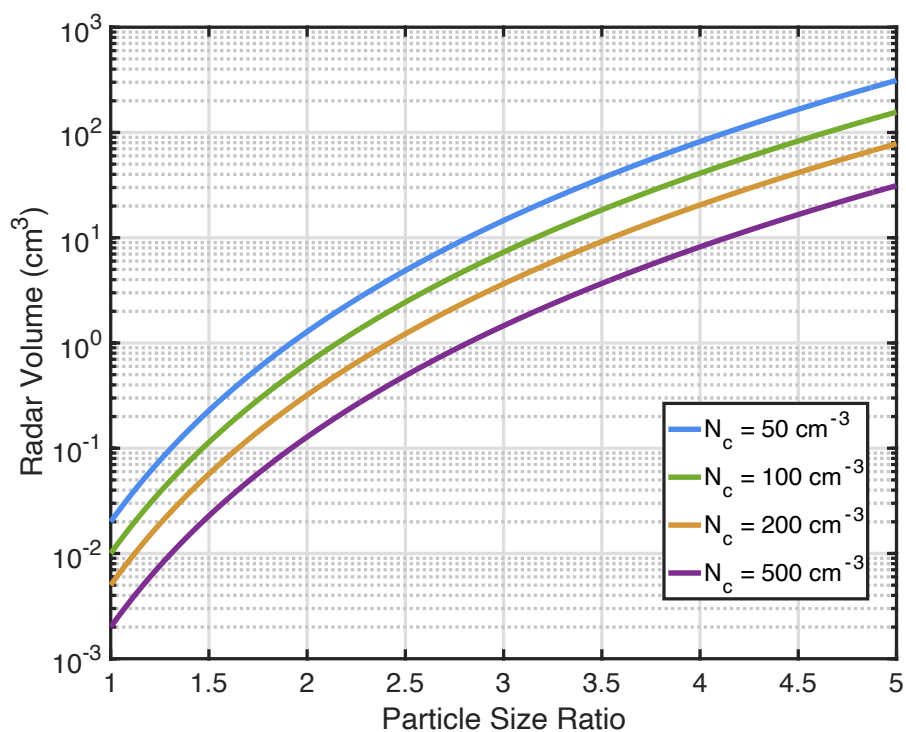
183

184   Figure 1: Radar observational volume for single-drizzle-drop detection as a function of particle

185   size ratio $x = \frac{D_d}{D_c}$. Lines of different color represent clouds number concentration (N_c): 50 cm^{-3}

186   (blue), 100 cm^{-3} (green), 200 cm^{-3} (yellow) and 500 cm^{-3} (purple).

187

188

189   3.2 Drizzle detection against an idealized cloud droplet background

190

191   In a realistic cloud chamber environment, we expect a population of cloud droplets with various

192   sizes that can be represented by a DSD. Particularly, when condensation and fallout are the main

193   sources and sinks for the evolution equation for the DSD, the DSD in the cloud chamber can be

194   approximately described by theoretically derived distributions (Saito et al., 2019;Chandrakar et al.,

195   2020;Krueger, 2020). Here we adapt the theoretical DSD formula derived by Krueger (2020) to

196   investigate the ability of a radar to detect a drizzle embryo present in a small sample volume under

197   different chamber environment conditions. To better represent the cloud DSD under different

198   environments, the analytical DSD is rearranged to be expressed as a function of liquid water

199   content (LWC$_c$; $g\ m^{-3}$) and number concentration (N_c; m^{-3}) as:

200

201
$$N(D_c) = \frac{2N_c D_c}{\pi^{1/2}} \left(\frac{4\Gamma\left(\frac{5}{4}\right)\pi^{\frac{1}{2}}\rho_l N_c}{3LWC_c} \right)^{2/3} \exp\left(-\left(\frac{4\Gamma\left(\frac{5}{4}\right)\pi^{\frac{1}{2}}\rho_l N_c}{3LWC_c} \right)^{\frac{4}{3}} \left(\frac{D_c}{2} \right)^4 \right) \quad (6)$$

202

203   where ρ_l is liquid water density ($g\ m^{-3}$), and D_c is cloud droplet diameter (m). $N(D_c)$ represents

204   the number concentration of cloud droplet for the given diameter ($cm^{-3}\ \mu m^{-1}$).

205

206   Here we define the minimal drizzle drop ($D_{d,min}$) as the size of particle with radar return power

207   equal to the total return power from cloud droplets in a given radar volume (V). Given the cloud

208   DSD described by Eq. 6, $D_{d,min}$ can be estimated as:

209

210
$$D_{d,min}^6 = \int V N(D_c) D_c^6 dD \quad (7)$$

211
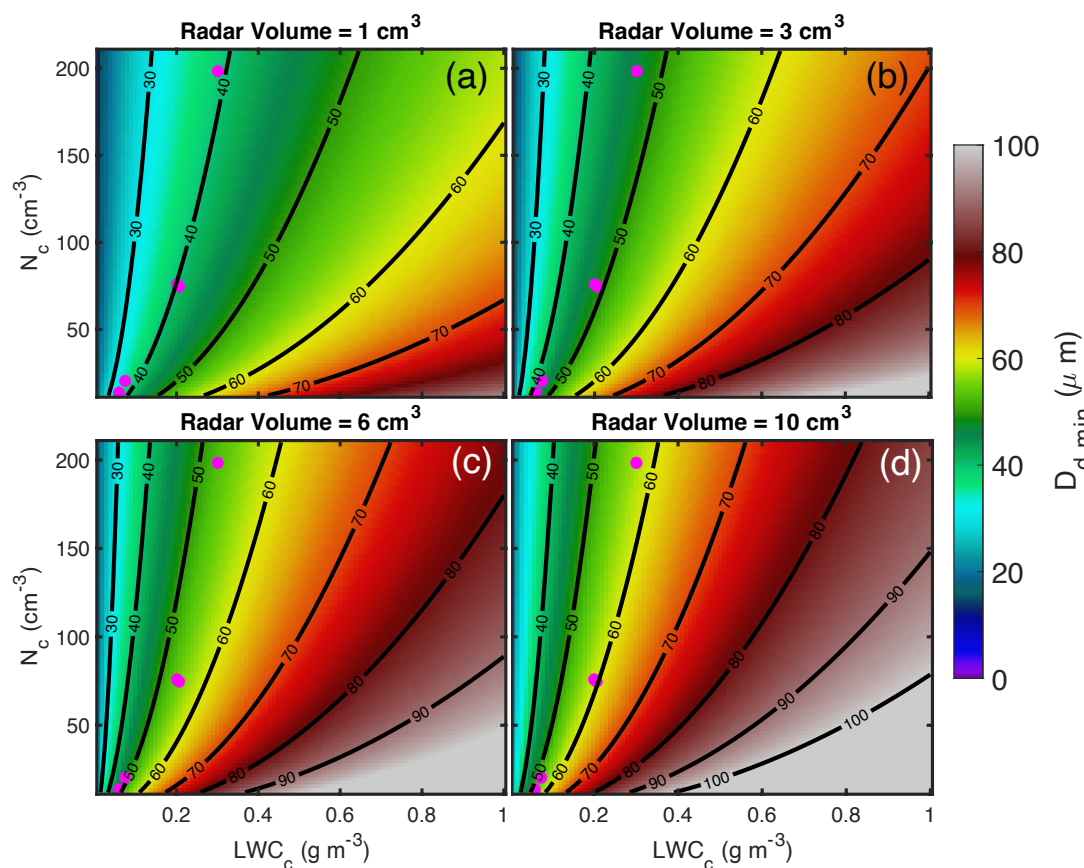
212   Figure2: The minimal detectable drizzle particle ($D_{d,min}$) under different LWC$_c$ and N_c conditions

213   with radar sampling volume of (a) 1 cm^3, (b) 3 cm^3, (c) 6 cm^3 and (d) 10 cm^3. The black lines are

214   the $D_{d,min}$ contour of 30 μm, 40 μm, 50 μm, 60 μm, 70 μm. The magenta dots indicate the LWC$_c$

215   and N_c observed in the Pi-cloud chamber.

216

217   Fig. 2 illustrates $D_{d,min}$ under different LWC$_c$ and N_c combinations for various radar volumes. For

218   a given steady-state cloud in a convection chamber (i.e., fixed LWC$_c$ and N_c), $D_{d,min}$ generally

219   increases as the radar volume increases. This is because larger radar volumes contain more cloud

220   droplets that produce stronger background power, thus only a larger drizzle particle with a higher

221   backscattering signal would be detectable. On the other hand, for a given radar observational

222   volume, $D_{d,min}$ is jointly determined by LWC$_c$ and N_c which are inversely proportional. As such,

223    $D_{d,min}$ increases rapidly with increasing LWC$_c$ but slightly decreases with increasing N_c. This

224   contrasting relationship is caused by a larger sensitivity of radar reflectivity to particle size than to

225   number concentration. Thus, increasing LWC$_c$ can increase mean cloud particle size and greatly

226   enhance the background power, leading to a larger detectable $D_{d,min}$. On the other side, when

227   LWC$_c$ is fixed, increasing cloud total number concentration tends to decrease particle size. The

228   reduced cloud particle size would reduce the backscattering power and more than compensate for

229   the power enhancement contributed from the increased number concentration.

230

231   It should be noted that the actual LWC$_c$ and N_c conditions in cloud chamber do not vary over the

232   full range shown in Fig. 2. Instead, the LWC$_c$ and N_c often exhibit a positive covariance

233   relationship. To understand the typical value of these two quantities in the chamber environment,

234   we refer to typical measurement data from the Pi Chamber (magenta dots in Fig. 2). The data are

235   from experiments conducted by Chandrakar et al. (2018). We can notice that for this specific

236   experiment set up, drizzle embryos with diameter ranging from 40 μm to 60 μm can be detected

237   using radar observational volume from 1 cm^3 to 10 cm^3.

238

239   The aforementioned estimation is conducted under the assumption that signal (drizzle) power is

240   equal to the background (cloud) power. In practice, to reduce the probability of detection false

241   alarms, the drizzle signal should be larger than the backgrounds. Here we define the signal to noise

242   ratio (SNR) to investigate the drizzle detectability in the chamber environment:

243

244
$$SNR = 10\,log10\left(\frac{D_d^6}{\int VP(D_c)D_c^6\,dD}\right). \quad\quad (8)$$

245

246   Fig. 3 shows the estimated SNR for four drizzle particles under varying LWC$_c$ and N_c conditions

247   with a radar volume of 1 cm^3. Generally, a smaller LWC$_c$ and a larger N_c correspond to a large

248   SNR, which is preferable for drizzle detection. If we arbitrarily choose SNR > 3 as the detection

249   threshold, to detect a drizzle drop with diameter of 50 μm in a radar volume of 1 cm^3 (Fig. 3c),

250   LWC$_c$ in the cloud chamber should be lower than 0.3 $g\ m^{-3}$ and N_c should be high than 90 cm^{-3}.

251   The required LWC$_c$ and N_c would be different for different drizzle particle targets: to detect drops

252   with diameter of 60 μm , LWC$_c$ should be lower than 0.5 $g\ m^{-3}$ and N_c should be higher than 90

253   cm^{-3}. It should be noted that although a drizzle drop is more likely to be detected by the radar at a

254   lower LWC_c, drizzle initiation is generally more likely to occur at a higher LWC_c because the

255   collision-coalescence rate is thought to be proportional to the square of LWC (Kostinski and Shaw,

256   2005). This suggests appropriate LWC_c and N_c combinations should be achieved such that drizzle

257   can form by the C-C process in a convection cloud chamber and it can also be detected by radar in

258   a small sampling volume. It is also noted that the results shown in Fig.3 are based on a radar

259   volume of 1 cm^3, and the estimated SNR would change if a different radar volume size is applied.

260   For instance, increasing the radar volume will enhance the background power thus decreasing the

261   SNR for the given cloud chamber environment.
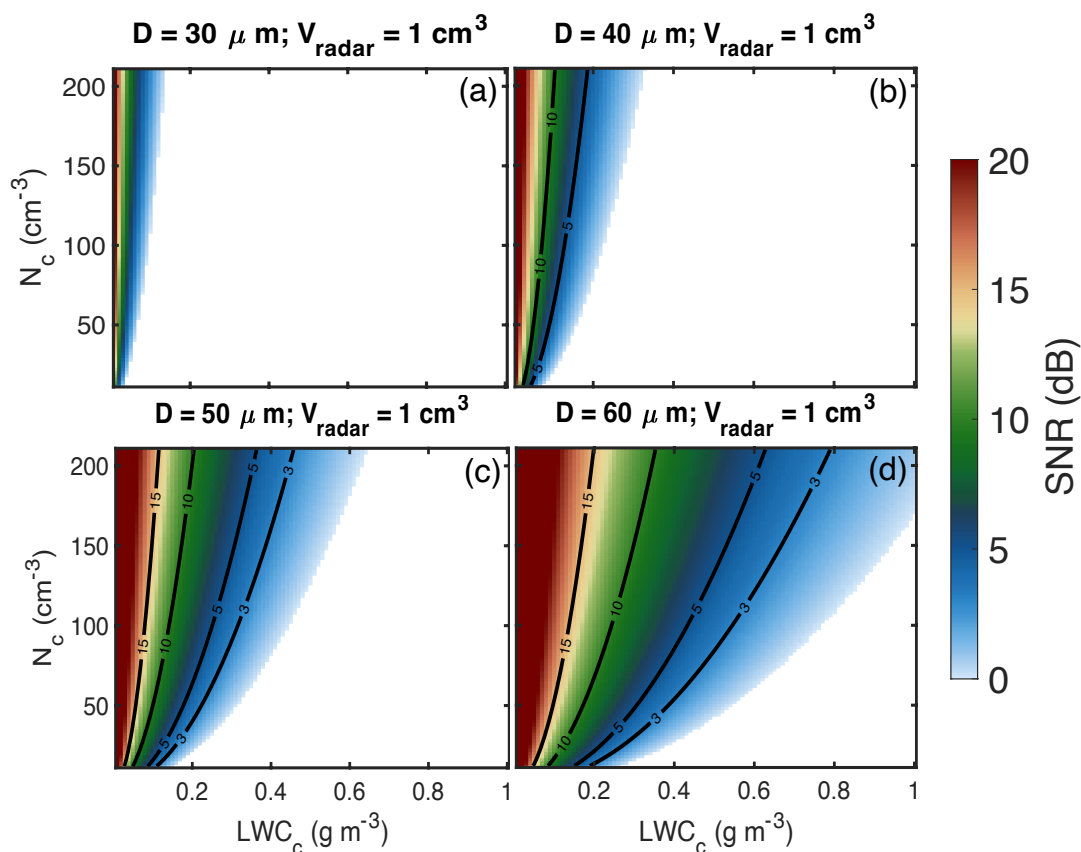
262

263   Figure 3: SNR of the drizzle signal under different LWC and N conditions in a 1 cm^3 radar sample

264   volume for drizzle diameters of 30 μm, 40 μm, 50 μm, 60 μm, and 70 μm. The black lines are

265   SNR contours of 3 dB, 5 dB, 10 dB and 15 dB. SNR lower than 0 is indicated as the blank region.

266

267

268   4. Probability of detection due to drizzle concentration

269

270   In the previous section, it was demonstrated that a radar with very small sampling volume ($\sim cm^3$)

271   can plausibly achieve the detection of single drizzle droplets against a cloud background signal.

272   On the other hand, the smaller the radar volume, the lower the probability of a drizzle particle

273   encountering the volume. To illustrate this trade-off scenario, we define the probability of drizzle

274   occurrence in the radar volume ($p(D_d)$) as:

275

276
$$p(D_d) = \begin{cases} 1, & VN(D_d)\Delta D \geq 1 \\ VN(D_d), & VN(D_d)\Delta D < 1 \end{cases} \tag{9}$$

277

278   Specifically, the product of V and $N(D_d)$ represents the expected number of drizzle drops in the

279   radar volume. If the product is smaller than 1, it indicates the probability of the occurrence of

280   drizzle particle in a given volume; while if the product is larger than 1, it means, statistically, at

281   least one drizzle drop with a diameter of D_d exists in the radar volume, and thus we set $p(D_d)$=1.

282
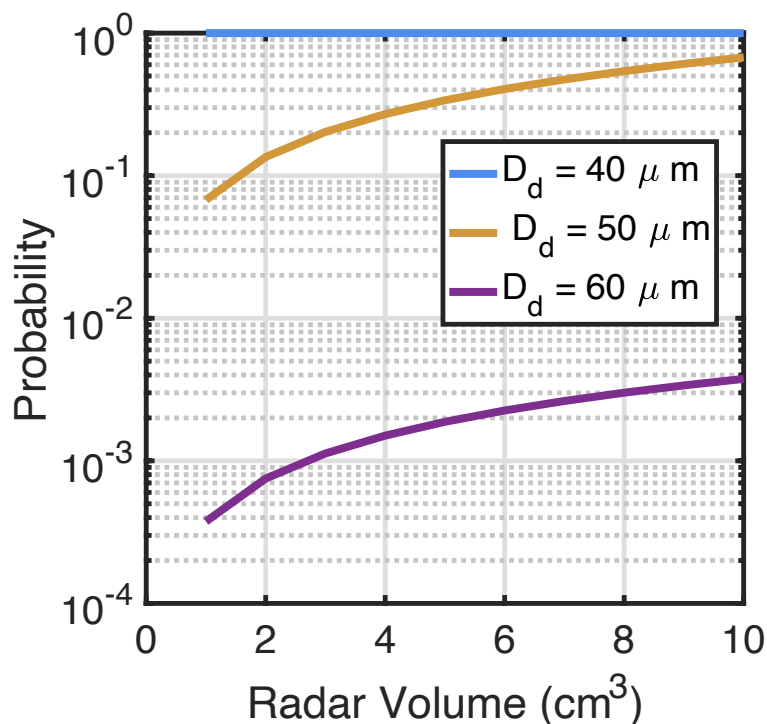
283

284

285 Figure 4: The probability of drizzle occurrence as a function of radar observational volume. The

286 blue, yellow, and purple lines indicate the drizzle particle with diameters of 40 μm, 50 μm, and 60

287 μm.

288

289 The probability of occurrence for three selected drizzle particles as a function of radar volume is

290 shown in Fig. 4. The *N(D)* in Eq. 9 is adapted from the size distribution described by Eq.6, with

291 LWC$_c$ and N_c set as 0.5 $g\ m^{-3}$ and 50 cm^{-3}, respectively. For these conditions, drizzle droplets with

292 a diameter of 40 μm have sufficiently high concentration to be on average always present in

293 volumes larger than 1 cm^3. For drizzle droplets with a diameter of 50 μm or 60 μm, their

294 concentration is low enough that their probability of being found in a 10 cm^3 volume is on average

295 below 1. It is also noticed that the occurrence probability is strongly sensitive to the particle size:

296 the probability of drizzle with 60 μm diameter occurring in the volume is almost two magnitudes

297 smaller than that for a particle with 50 μm diameter. A smaller drizzle occurrence in the volume

298 indicates that a larger number of radar samples would be required to find one particle, leading to

299 a longer observational time.

300

301 The probability of a drizzle drop to be in the radar sampling volume or passing through the radar

302 volume within a finite time period should be an important consideration for a practical

303 measurement system. Fig. 5 shows the probability of the occurrence of drizzle particle under

304 different chamber environments same as Fig. 3. The blank region in Fig. 5 indicates the

305 corresponding SNR shown in Fig. 3 is lower than 0 (i.e., cannot be detected by the radar even they

306 exist in the sampling volume). Generally, it is noticed that the probability of occurrence differs in

307 various chamber environment for different droplet size: large droplets have lower occurrence

308 probability under small LWC and high N conditions.
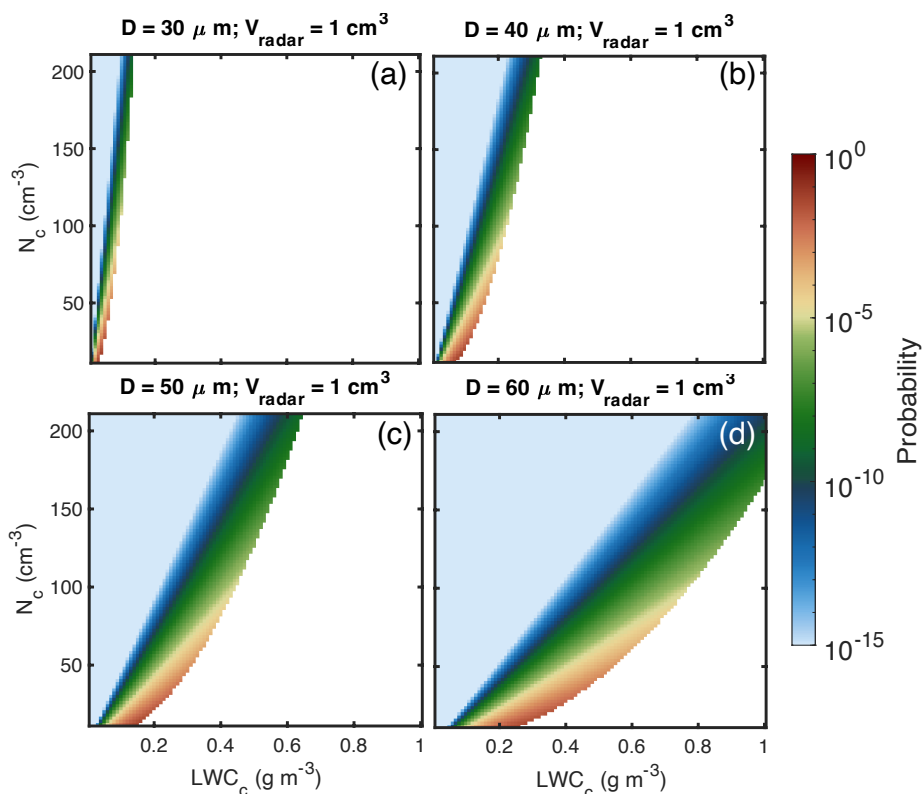
309 Figure 5: Drizzle occurrence probability under different LWC and N conditions for a 1 cm^3 radar

310 volume with particle diameter of (a) 30 μm, (b) 40 μm, (c) 50 μm, and (d) 60 μm. The blank region

311 indicates that the associated SNR is smaller than 0 (Fig. 3).

312

313 Comparison of Fig. 3 and Fig. 5 reveals that conditions that favor high radar SNR (i.e., larger drops

314 or smaller radar sampling volume) are associated with a lower probability of occurrence of the

315 drizzle droplet in the radar volume and subsequently increase the radar sampling time. For example,

316 to detect a drizzle particle of 50 μm diameter under the condition of LWC$_c$ and N_c of 0.3 $g\ m^{-3}$, 90

317 cm^{-3}, the particle occurrence probability is on the magnitude of 10^{-8} (Fig. 5c) for SNR equals to 3

318 (Fig. 3c). A 1 dB enhancement of SNR threshold would decrease the occurrence probability to 10^{-11}.

319 This implies that on average, a volume of air equal to 10^{11} times the size of the radar sampling

320 volume needs to be sampled before a drizzle droplet will be detected. Assuming an air mean flow

321 within the cloud chamber of 1 m s^{-1}, this implies that a radar sampling volume with a typical

322 dimension of 1 cm will be updated (through advection) 100 times per second. If the radar is

323 sampling along 1000 range gates (i.e. assuming a chamber with height of 10 m), this suggests that

324 the radar can sample a volume equal to 10^5 its radar sampling volume each second. To reach the

325 average required sampling volume (10^{11}), it will take 10^6 seconds or 11.5 days. This is an

326 unrealistically long observational time. For practical application, we want to work with sampling

327 configurations that will not require to sample more than 10^9 times the radar sampling volume (~10s

328 of minutes).

329

330 Another factor to consider in estimating the probability of drizzle occurrence with a certain

331 diameter in a specific volume is the realism of using Eq. 6 for describing the $N(D)$ in a cloud

332 chamber. Eq. 6 describes the cloud droplet distribution controlled by the condensation process

333 alone, thus the results may underestimate the actual drizzle occurrence as condensation is

334 inefficient to produce large drizzle particle. In nature or in a large convection cloud chamber, the

335 C-C mechanism is expected to be a more efficient process to increase the size and concentration

336 of drizzle droplets.

337

338 Here we apply the ClusColl model to demonstrate that Fig. 4 and Fig. 5 may underestimate the

339 drizzle occurrence probability with the collision-coalescence process being activate. ClusColl is a

340 simulation method for describing droplet motions and collisions in turbulent flows (Krueger and

341 Kerstein, 2018). ClusColl simulates the movement of individual droplets in a vertical column due

342 to turbulence and gravitational sedimentation. The unique capability of the ClusColl model is its

343 capability to efficiently simulate the droplet collisions and coalescence process. Fig. 6 shows the

344 simulated DSD with and without the collision-coalescence process for a 10-*m*-height cloud

345 chamber and with cloud number concentration of 100 cm^{-3}. The temperature difference between

346 top and bottom walls is 40 °C. Noticeable differences can be identified at the right tail of the

347 distribution, particularly for droplet diameter larger than 40 μm: more larger droplets are generated

348 if the collision-coalescence process is active. The higher concentration of large drops results in a

349 significantly shorter waiting time for detection compared to what was calculated for the

350 condensation-only examples given in the earlier part. For instance, for the generated particle with

351 diameter of 50 μm, the C-C process can generate number concentration more than 100 higher than

352 the one without C-C process included. Reviewing the earlier estimation, to detect drizzle particle

353 with diameter of 50 μm with SNR higher than 4, the required 10^6 s becomes 10^4 s which is

354 approximately 3 hours, which is much more achievable for laboratory experiment. Thus, the

355 estimation based on the condensation-only distribution (Eq. 6) is the most-conservative scenario.

356 The actual radar measurement time would likely to be much shorter when the C-C process is

357 activated.

358

359
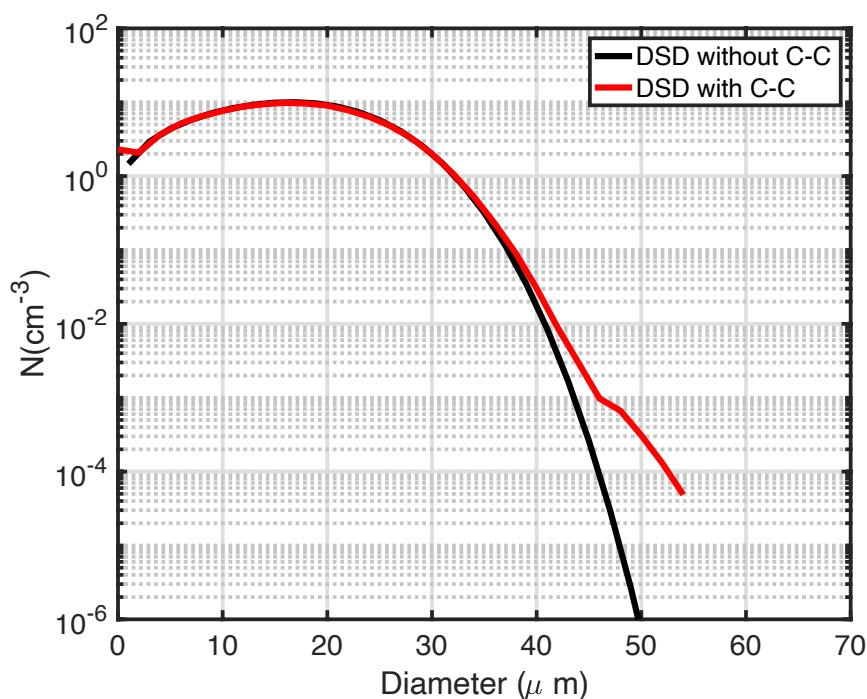
360

361

362 Figure 6: DSD simulated from the ClusColl model with (red line) and without (black line) droplet

363 growth by collision-coalescence. In both cases, growth by condensation in a uniform

364 supersaturation field, and removal by size-dependent droplet sedimentation are calculated.

365 Therefore, the black line is described by the distribution given by Equation 6.

366

367

368

369   5. Evaluation from cloud chamber observations

370

371 In a cloud chamber and in the real atmosphere, the DSD in the radar sampling volume is expected

372 to be time dependent due to turbulent fluctuations. To better quantify the particle backscattering

373 power and its fluctuation in a small volume, observations made in the Pi Chamber using a

374 holographic system (Holo-Pi) are used. Holo-Pi uses the principle of in-line digital holography to

375   measure the spatial distribution and sizes of cloud particles (Fugal and Shaw, 2009;Beals et al.,

376   2015), and is specifically designed for the Pi-chamber environment (Desai et al., 2018). In contrast

377   to the typical measurement strategy of single particle detections requiring time averaging, Holo-

378   Pi captures instantaneous snapshots of all cloud droplets in the sample volume of 3.6 cm^3 (0.6 cm

379   × 0.6 cm × 10 cm) and is well suited to measure the temporal variations of cloud droplet

380   populations within a sample volume similar to plausible radar sample volumes. The inability to

381   resolve the smallest cloud droplets in the size distribution is not expected to be a significant

382   limitation as the backscattering radar power is more sensitive to larger particle diameters. For the

383   results presented here, cloud droplets are formed in the Pi Chamber by activation of size-selected

384   sodium chloride aerosol particles (dry particle diameter ≈ 130 nm) injected into a supersaturated

385   turbulent flow sustained by an unstable temperature difference of 20 K. An illustration of the 3D

386   view of the cloud droplets measured by Holo-Pi at different time instants in the Pi-chamber is

387   shown in Fig. 7. The sample volume used for our calculations is limited to a vertical extent of 5

388   cm as particle detectability falls off beyond this point; this results in a total sample volume of 1.8

389   cm^3. The Holo-Pi system is set up to capture a hologram every 10 seconds during a 720-s period.

390   For the optical configuration used here, the Holo-Pi has a lower size resolution of 12 μm

391   throughout its sample volume.

392

393

394

395
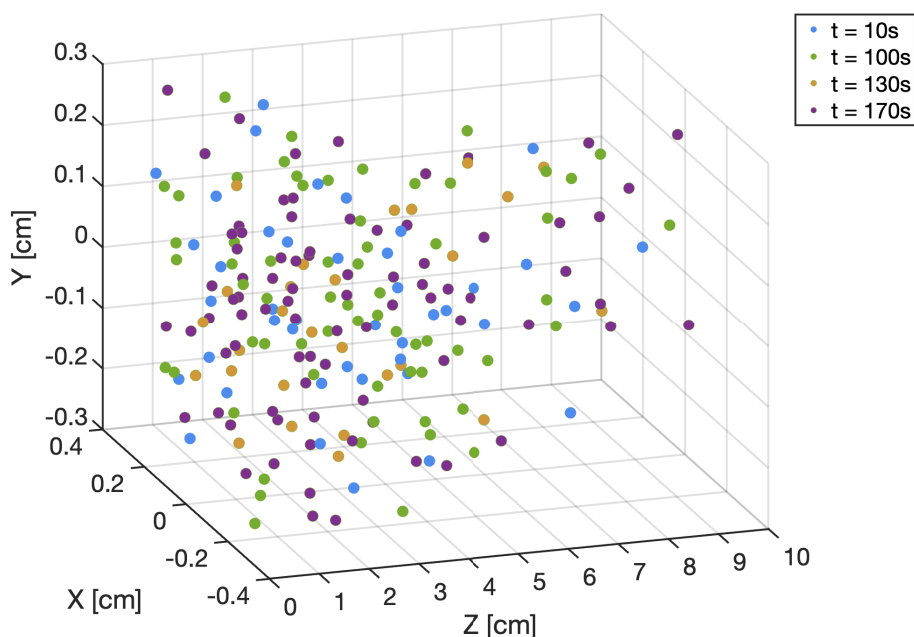
Figure 7: A 3D view of the particle locations observed by Holo-Pi in the Pi Chamber. Different colors represent observations taken at different timesteps.

398

The Holo-Pi observational volume is divided into five sub volumes with the cross section of 0.36 cm^2 and the depth increasing from 1 to 5 cm with an increment of 1 cm, thus, corresponding to a volume of 0.36, 0.72, 1.08, 1.44 and 1.8 cm^3. Within each sub-volume at each time step, the total backscattering cross section for the detected droplets is estimated using a THz radar with wavelength of 0.44 mm. The calculated radar backscattering cross section as a function of volume size is shown in Fig. 8. Similar to the previous estimation, we see that the background power increases with volume size due to the increment of cloud droplets. Importantly, the uncertainty bars shown in Fig. 8 represent the standard deviation of the backscattering cross section during the observational time, which indicates the background power fluctuations. We notice that the cloud distribution in a small radar sampling volume is highly heterogeneous in time, and the magnitude of the background fluctuation varies by approximately a factor of 10. In order to detect drizzle drops, the backscattering power of the drizzle drop should be larger than the range of background

411   fluctuations. For example, a radar volume smaller than 0.36 cm^3 should be utilized to detect a

412   droplet with a diameter larger than 22 μm, and a radar sampling volume smaller than 1 cm^3 is

413   needed to detect droplet with diameter larger than 30 μm for this particular Pi Chamber experiment

414   set up.

415
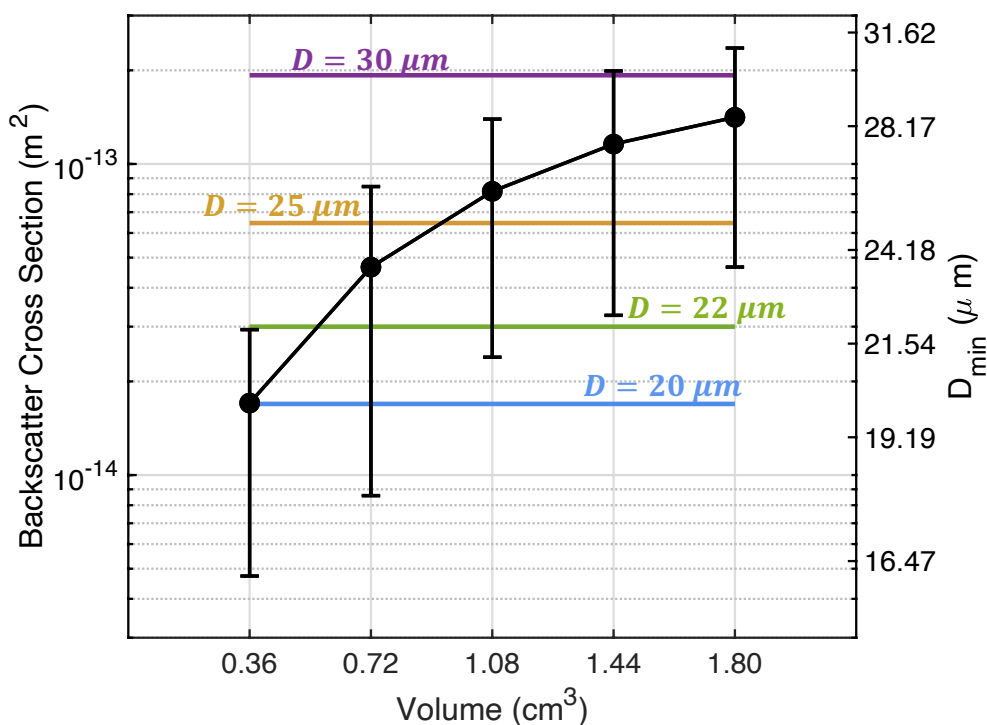
416

417   Figure 8: Dots and uncertainty bars indicate the mean and standard deviation of the total

418   backscattering cross-section (with units of m^2) of droplets measured in different volumes by Holo-

419   Pi during the observational period. The right axis and the horizontal lines represent the diameter

420   of a single drizzle drop with backscattering power equivalent to the background.

421 To further demonstrate the single drizzle detection concept using a small radar volume, a pseudo-
422 radar observation experiment is conducted based on the Holo-Pi measurements. The Holo-Pi
423 observational volume is divided into 4 sub-volumes indicated as different lines shown in Fig. 9. In
424 each volume, we consider the mean radar backscattering power from all cloud particles sampled
425 during the observational period as the background noise, and the power estimated at each time step
426 as the signal, such that the SNR as a function of observation time is estimated. To simulate the
427 drizzle occurring events, artificial drizzle droplets with diameter of 30 μm, 40 μm, 50 μm are
428 added to the volume at 200 s, 400 s, and 600 s, respectively, and the associated SNR is estimated.
429 Fig. 9 shows a clear SNR enhancement when the drizzle droplets are added. The signal
430 enhancement is more significant when using a small sampling volume and for larger drizzle drop
431 diameter, which is consistent with the theoretical estimation in Sec. 3. For instance, a drizzle drop
432 with a diameter of 50 μm can have a SNR of 23 dB with a volume of 0.36 cm^3 while it has a SNR
433 of 15 dB with a volume of 1.44 cm^3. For a drizzle drop of 30 μm, the SNR with a volume of 0.36
434 cm^3 can reach to 10 dB, which is an adequate SNR value for radar detection, while with a volume
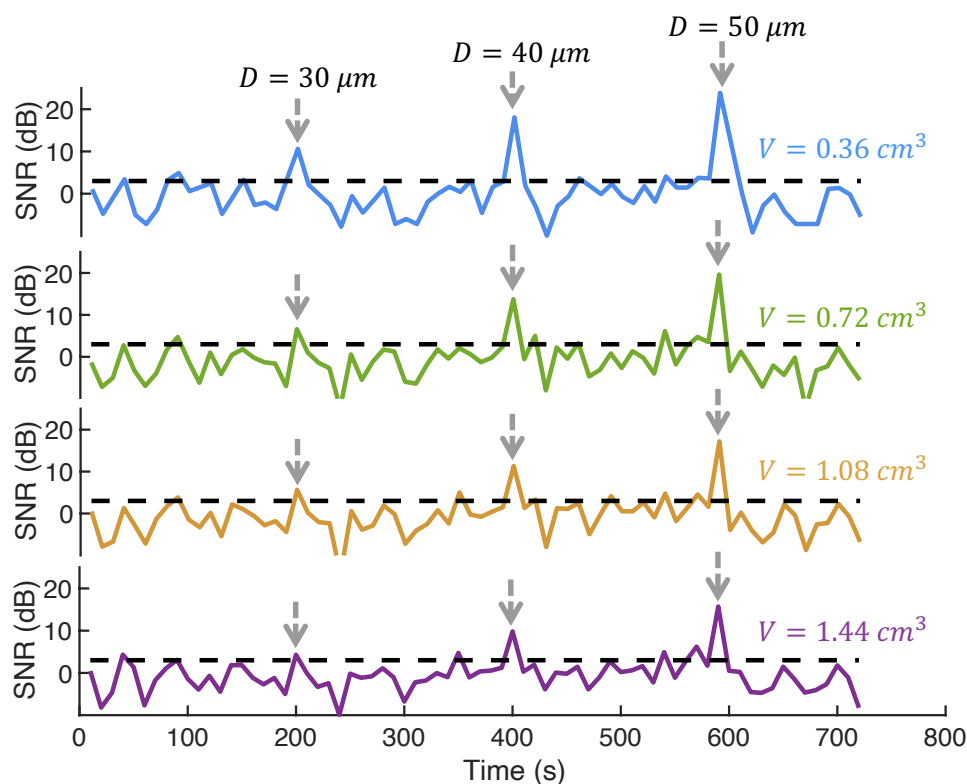
435   of 1.44 cm^3, the drizzle drop SNR is overwhelmed by background fluctuation and it is unable to

436   be detected.

437

438   Figure 9: Simulated SNR of radar measurements during the Holo-Pi observational period using

439   four sampling volumes: 0.36 cm^3 (blue line), 0.72 cm^3 (green line), 1.08 cm^3 (yellow line) and

440   1.44 cm^3 (purple line). The grey arrows indicate an artificial drizzle particle is added at the

441   indicated time step. The black dashed line indicates a SNR of 3, which is used as a threshold to

442   distinguish the signal (drizzle) from the background (clouds) in Fig. 3.

443

444   6. Summary

445

446   Recent simulation results suggest that drizzle initiation could occur in a large convection-cloud

447   chamber. Such a facility would provide measurements in a controlled environment that can

448   advance our understanding of warm rain formation in clouds. One of the critical measurements in

449   a large convection-cloud chamber is the detection of low-concentration drizzle droplets in the

450   presence of numerous cloud droplets. Early in the drizzle initiation, those drizzle drops are rare

451   and in-homogeneously distributed in the chamber, presenting a significant detection challenge for

452   conventional in-situ probes. Here, the potential of a radar with ultra-fine sampling volume for

453   drizzle detection is investigated. It was demonstrated that if the radar sampling volume becomes

454   orders of magnitude smaller (e.g., several cm^3), compared to those typically available in research

455   radars (~10^3-10^6 m^3), isolated drizzle particles can be detected against the cloud background signal.

456   This concept is based on the notion that the SNR of point targets (i.e., drizzle droplet) is

457   independent of the radar sampling volume while the SNR of background (i.e., high concentration

458   cloud droplets) scales with the sampling volume.

459

460   A theoretical DSD was adapted to represent the distribution of cloud droplets in a convection cloud

461   chamber and to estimate properties of a detectable drizzle particle. It was shown that the minimum

462   size of an isolated drizzle droplet that can be detected with such a radar depended on the radar

463   sampling volume and the strength of the background signal (i.e., cloud droplets radar return), that

464   in turn, depends on LWC and N_c. To minimize the false alarm drizzle detection, we require that

465   the backscattering power from a drizzle particle should be larger than the backscattered power

466 contributed from the cloud particles (SNR>1). It is demonstrated that the application of a small

467 radar volume can significantly enhance SNR under a given chamber environment. On the other

468 hand, the smaller the radar sampling volume the lower the probability of an isolated drizzle droplet

469 to be sampled. Thus, the determination of the radar volume for drizzle detection should account

470 for the size of drizzle particle of interest, the environment conditions that favor drizzle initiation

471 and the required observational time.

472

473 In addition to analytical estimates, real observations from the MTU Pi convection-cloud chamber

474 are used to demonstrate the single drizzle particle detection framework. The Holo-Pi system(Desai

475 et al., 2018) is applied to provide detailed 3D imaging of the cloud particles in the cloud chamber,

476 from which the fluctuations of the backscattering power in a small volume can be well estimated.

477 Generally, the observational results are consistent with the theoretical estimation showing that the

478 background power is decreased and the ability to detect drizzle particles is enhanced as radar

479 sample volume is decreased. It is also noticed that the magnitude of the background fluctuation is

480 comparable to the mean power, which indicate that the distribution of cloud droplets is highly

481 inhomogeneous in the small volume. Thus, the power from a drizzle particle should at least

482 dominate the background power fluctuation in order to be detected. With the cloud chamber

483 environment from the experiment, drizzle particles with diameter larger than 30 μm can be

484 confidently detected using a radar sampling volume of 1 cm^3 or lower.

485

486 The key remaining question is the technological feasibility of building a radar that can operate

487 within a box (large convection cloud chamber) and achieve the required ultra-fine range resolution.

488 In fact, the effort of using "small" radar volumes for single particle detection has already been

489 achieved in previous studies. For example, Schmidt et al. (2012) utilized a C-band radar with a 14-

490 m^3 observational volume and successfully detected the trajectories of rain droplet with diameter

491 down to 0.5 mm. In our case, the required radar sampling volume for drizzle detection is much

492 smaller (with several cm^3). Such ultra-fine range resolution can be achieved using a THz radar

493 operating at 340 or 680 GHz that can support wide bandwidth waveforms and thus enable sub-

494 centimeter range resolution (Cooper and Chattopadhyay, 2014). If the radar operates at a very high

495 carrier frequency (THz) it can afford a very wide bandwidth for pulse modulation. In this case, the

496 range resolution in not dictated by the pulse length but from the radar bandwidth (Cooper and

497   Chattopadhyay, 2014). The ultra-fine range resolution along with a reflector that minimizes the

498   angular spread of the radar beam can result in radar sampling volumes of a few cm^3. Such radar

499   imaging capabilities have been extensively used for security screening at airports, for example. In

500   our context, additional complexity is introduced by the fact that this radar needs to operate in a

501   chamber with typical dimension of ~ 10 m. These technical design issues will be the focus of a

502   follow-up paper study that will include real observations of drizzle droplets from a THz radar

503   system.

504

505   To conclude, we outline three issues that will need to be properly addressed before a radar can be

506   applied to the drizzle-detection problem in a cloud chamber:

507

508   1) Does the radar have enough sensitivity to detect a single drizzle particle? With the

509   development of the THz technology, radar with centimeter resolution is achievable,

510   however, the currently developed THz radars are mainly used to detect relatively hard

511   targets that do not require ultra-high sensitivity. For the purpose of drizzle detection,

512   however, the backscattering cross-section is on the order of 10^{-13} m^2; such lower receiving

513   power would require the radar to have a much higher transmitting power or a larger antenna

514   size. Fortunately, an advantage for the drizzle detection in a cloud chamber is that the radar

515   detection range is only several meters depending on the size of the chamber. According to

516   Eq. 1, radar receiving power is inversely proportional to the fourth power of the target

517   distance. Thus, the small detection range may greatly relieve the demand for high

518   sensitivity in the radar design. In addition, recent advancements in THz transmitters allow

519   us to utilize higher power output transmitter (~50 to 200 mW) at THz frequencies such as

520   340 GHz.

521

522   2) What are the appropriate radar sampling strategies for drizzle detection in a cloud chamber

523   facility? Most of the cloud radars applied in the atmosphere are vertically pointing and can

524   provide continuous observation at a given location along the radar beam. However as

525   discussed in the paper, drizzle occurrence in the chamber is extremely rare and

526   inhomogeneous in space and time. If the radar is vertically pointing, with the radar beam

527   of several cm width, it may wait significant time for the radar to detect one drizzle drop.

528   Adding a scanning capability to the radar may provide a more efficient way to observe and
529   detect drizzle in the cloud chamber.
530
531   3) How to eliminate or reduce the degradation effect of the chamber environment on a radar
532   signal? In particular, the cloud chamber is a humid environment with liquid particles
533   continually falling towards the bottom. Accumulation of water on the radar antenna can
534   also severally attenuate the transmitting power and degrade the radar detectability.
535   Furthermore, the chamber walls and the in-situ instruments mounted inside would produce
536   strong backscattering signals and pollute the backscattering signal from hydrometeors.
537   Thus, the design of the radar should also account for radar instrument design and sampling
538   strategies that minimize these noise sources so that the best possible detection capability
539   can be achieved.
540
541   In short, this paper demonstrates the conceptual feasibility of THz radars for rare drizzle detection
542   in a laboratory context. Undoubtedly, the development of a high-resolution radar for drizzle
543   detection in a cloud chamber needs close collaborations between cloud physics scientists and radar
544   engineers moving forward.
545

546   **Competing interests.**

547   **P. K.** is an associate editor of AMT.
548   The authors have no other competing interests to declare.
549
550   **Code/Data availability**

551   The codes and observations used to conduct all the analyses in this study are available upon
552   request.
553
554

Author contributions

Zeen Zhu conceptualized and implemented the method, performed the analysis, produced the figures, and wrote the initial draft of the manuscript. Pavlos Kollias and Fan Yang contributed to the conceptualization and provide guidance on the analysis. Raymond A. Shaw and Alex B. Kostinski contributed to the simplified model described in Section 3.1. Steve Krueger provided the ClusColl model. Nithin Allwayin provided the Holo-Pi measurements from the Pi Chamber. All authors read the manuscript draft and contributed comments and manuscript editing.

Acknowledgements

Authors from Brookhaven National Laboratory were supported by the Office of Biological and Environmental Research in the Department of Energy, Office of Science, through the United States Department of Energy Contract No. DE-SC0012704. Authors from Michigan Technological University and from Stony Brook University (subaward 2105003Z8) acknowledge support from National Science Foundation award AGS-2133229. A. Kostinski, S. Krueger, R. Shaw, and F. Yang accomplished some of this work during a visit at the Kavli Institute for Theoretical Physics as part of the Multiphase Flows in Geophysics and the Environment program. KITP is supported in part by National Science Foundation under grant number PHY-1748958. We also want to thank Dr. Ken Cooper for the constructive discussion and for providing feedback to the manuscript.

586

Reference

587

588

589 Acquistapace, C., Kneifel, S., Löhnert, U., Kollias, P., Maahn, M., and Bauer-Pfundstein, M.:
590 Optimizing observations of drizzle onset with millimeter-wavelength radars, Atmospheric
591 Measurement Techniques, 10, 1783-1802, 2017.

592 Battan, L. J.: Radar observation of the atmosphere, 1973.

593 Beals, M. A., Fugal, J. P., Shaw, R. A., Lu, J., Spuler, S. M., and Stith, J. L.: Holographic
594 measurements of inhomogeneous cloud mixing at the centimeter scale, Science, 350, 87-90,
595 2015.

596 Chandrakar, K., Cantrell, W., Kostinski, A., and Shaw, R.: Data supporting the paper" Dispersion
597 aerosol indirect effect in turbulent clouds: laboratory measurements of effective radius", 2018.

598 Chandrakar, K. K., Saito, I., Yang, F., Cantrell, W., Gotoh, T., and Shaw, R. A.: Droplet size
599 distributions in turbulent clouds: Experimental evaluation of theoretical distributions, Quarterly
600 Journal of the Royal Meteorological Society, 146, 483-504, 2020.

601 Chang, K., Bench, J., Brege, M., Cantrell, W., Chandrakar, K., Ciochetto, D., Mazzoleni, C.,
602 Mazzoleni, L., Niedermeier, D., and Shaw, R.: A laboratory facility to study gas–aerosol–cloud
603 interactions in a turbulent environment: The Π chamber, Bulletin of the American Meteorological
604 Society, 97, 2343-2358, 2016.

605 Comstock, K. K., Wood, R., Yuter, S. E., and Bretherton, C. S.: Reflectivity and rain rate in and
606 below drizzling stratocumulus, Quarterly Journal of the Royal Meteorological Society: A journal
607 of the atmospheric sciences, applied meteorology and physical oceanography, 130, 2891-2918,
608 2004.

609 Cooper, K. B., and Chattopadhyay, G.: Submillimeter-wave radar: Solid-state system design and
610 applications, IEEE microwave magazine, 15, 51-67, 2014.

611 Desai, N., Chandrakar, K. K., Chang, K., Cantrell, W., and Shaw, R.: Influence of microphysical
612 variability on stochastic condensation in a turbulent laboratory cloud, Journal of the Atmospheric
613 Sciences, 75, 189-201, 2018.

Feingold, G., Cotton, W. R., Kreidenweis, S. M., and Davis, J. T.: The impact of giant cloud condensation nuclei on drizzle formation in stratocumulus: Implications for cloud radiative properties, Journal of the atmospheric sciences, 56, 4100-4117, 1999.

Frisch, A., Fairall, C., and Snider, J.: Measurement of stratus cloud and drizzle parameters in ASTEX with a Kα-band Doppler radar and a microwave radiometer, Journal of the Atmospheric Sciences, 52, 2788-2799, 1995.

Fugal, J., and Shaw, R.: Cloud particle size distributions measured with an airborne digital in-line holographic instrument, Atmospheric Measurement Techniques, 2, 259-271, 2009.

Johnson, D. B.: The role of giant and ultragiant aerosol particles in warm rain initiation, Journal of Atmospheric Sciences, 39, 448-460, 1982.

Kollias, Clothiaux, E., Miller, M., Albrecht, B., Stephens, G., and Ackerman, T.: Millimeter-wavelength radars: New frontier in atmospheric cloud and precipitation research, Bulletin of the American Meteorological Society, 88, 1608-1624, 2007.

Kollias, Remillard, J., Luke, E., and Szyrmer, W.: Cloud radar Doppler spectra in drizzling stratiform clouds: 1. Forward modeling and remote sensing applications, Journal of Geophysical Research-Atmospheres, 116, 10.1029/2010jd015237, 2011.

Kollias, Clothiaux, E. E., Ackerman, T. P., Albrecht, B. A., Widener, K. B., Moran, K. P., Luke, E. P., Johnson, K. L., Bharadwaj, N., and Mead, J. B.: Development and applications of ARM millimeter-wavelength cloud radars, Meteorological Monographs, 57, 17.11-17.19, 2016.

Kostinski, A. B., and Shaw, R. A.: Fluctuations and luck in droplet growth by coalescence, Bulletin of the American Meteorological Society, 86, 235-244, 2005.

Krueger, S. K., and Kerstein, A. R.: An economical model for simulating turbulence enhancement of droplet collisions and coalescence, Journal of Advances in Modeling Earth Systems, 10, 1858-1881, 2018.

Krueger, S. K.: Equilibrium droplet size distributions in a turbulent cloud chamber with uniform supersaturation, 2020.

Liu, Y., Geerts, B., Miller, M., Daum, P., and McGraw, R.: Threshold radar reflectivity for drizzling clouds, Geophysical research letters, 35, 2008.

642 Pinsky, and Khain, A.: Turbulence effects on droplet growth and size distribution in clouds—A

643 review, Journal of aerosol science, 28, 1177-1214, 1997.

644 Saito, I., Gotoh, T., and Watanabe, T.: Broadening of cloud droplet size distributions by

645 condensation in turbulence, Journal of the Meteorological Society of Japan. Ser. II, 2019.

646 Schmidt, J. M., Flatau, P. J., Harasti, P. R., Yates, R. D., Littleton, R., Pritchard, M. S., Fischer, J. M.,

647 Fischer, E. J., Kohri, W. J., and Vetter, J. R.: Radar observations of individual rain drops in the free

648 atmosphere, Proceedings of the National Academy of Sciences, 109, 9293-9298, 2012.

649 Shaw, R. A.: Particle-turbulence interactions in atmospheric clouds, Annual Review of Fluid

650 Mechanics, 35, 183-227, 2003.

651 Shaw, R. A., Cantrell, W., Chen, S., Chuang, P., Donahue, N., Feingold, G., Kollias, P., Korolev, A.,

652 Kreidenweis, S., and Krueger, S.: Cloud–aerosol–turbulence interactions: Science priorities and

653 concepts for a large-scale laboratory facility, Bulletin of the American Meteorological Society,

654 101, E1026-E1035, 2020.

655 Thomas, S., Yang, F., Ovchinnikov, M., Cantrell, W., and Shaw, R. A.: Scaling of turbulence and

656 microphysics in a convection–cloud chamber of varying height, Journal of Advances in Modeling

657 Earth Systems, 15, e2022MS003304, 2023.

658 Wood: Stratocumulus Clouds, Monthly Weather Review, 140, 2373-2423, 10.1175/mwr-d-11-

659 00121.1, 2012.

660 Yau, M. K., and Rogers, R. R.: A short course in cloud physics, Elsevier, 1996.

661 Zhu, Z., Kollias, P., Luke, E., and Yang, F.: New insights on the prevalence of drizzle in marine

662 stratocumulus clouds based on a machine learning algorithm applied to radar Doppler spectra,

663 Atmospheric Chemistry and Physics, 22, 7405-7416, 2022.

664